Extending single mode performance of all-solid large-mode-area single trench fiber

D. Jain,* Y. Jung, M. Nunez-Velazquez, and J. K. Sahu

Optoelectronics Research Center, University of Southampton, Southampton SO17 1BJ, United Kingdom

Abstract: We report a novel "single trench fiber" design for mode area scaling of the fundamental mode while offering effective single mode operation for a compact fiber laser device. This fiber design allows very high suppression of the higher order modes by offering high loss and power delocalization. It has the advantages of low cost and easy fabrication thanks to all solid fiber design, cylindrical symmetry, and higher refractive index of core as that of the cladding. A Yb-doped single trench fiber with a 40μm core diameter has been fabricated from modified chemical vapor deposition process in conjunction with solution-doping offering an effective mode area of as large as ~1,000μm^2 at 1060nm for the bend radius of 20cm. Detailed characterizations confirm a robust single mode behavior of the fiber. Comparative analysis with other fiber designs shows significant performance enhancement of effective single mode operation suitable for fiber laser applications.

OCIS codes: (060.2280) Fiber design and manufacturing; (140.3510) Fiber lasers.

References and links

1. C. Jauregui, J. Limpert, and A. Tunnermann, "High-power fiber lasers," [Invited], Nat. Photonics **7**, 861-867 (2013).
2. M. N. Zervas and C. A. Codemard, "High power fiber lasers: A Review," [Invited], IEEE J. Sel. Top. Quantum Eletron. **20,** 0904123 (2014).
3. G. P. Agrawal, *Nonlinear Fiber Optics*, 4th ed. (Academic, 2007).
4. M.-J. Li, X. Chen, A. Liu, S. Gray, J. Wang, D. T. Walton, and L. A. Zenteno, "Limit of effective area for single-mode operation in step-index large mode area laser fibers," J. Lightwave Technol. **27**, 3010-3016 (2009).
5. J. Limpert, A. Liem, M. Reich, T. Schreiber, S. Nolte, H. Zellmer, and A. Tunnermann, "Low-nonlinearity single-transverse-mode ytterbium-doped photonic crystal fiber amplifier," Opt. Exp. **12**, 1313-1319 (2004).
6. G. Gu, F. Kong, T. W. Hawkins, P. Foy, K. Wei, B. Samson, and L. Dong, "Impact of fiber outer boundaries on leaky mode losses in leakage channel fibers," Opt. Exp. **21**, 24039-24048 (2013).
7. R. A. Barankov, K. Wei, B. Samson, and S. Ramachandran, "Resonant bend loss in leakage channel fibers," Opt. Lett. **37**, 3147-3149 (2012).
8. T. T. Alkeskjold, "Large-mode-area ytterbium-doped fiber amplifier with distributed narrow spectral filtering and reduced bend sensitivity," Opt. Exp. **17**, 16394-16405 (2009).
9. E. M. Dianov, M. E. Likhachev, and S. Fevrier, "Solid-core photonic bandgap fibers for high-power fiber lasers," IEEE J. Sel. Top. Quant. Electron. **15**, 20-29 (2009).
10. G. Gu, F. Kong, T. Hawkins, J. Parsons, M. Jones, C. Dunn, M. T. Kalichevsky-Dong, K. Saitoh, and L. Dong, "Ytterbium-doped large-mode-area all-solid photonic bandgap fiber lasers" Opt. Exp. **22**, 13962-13968 (2014).
11. X. Ma, C. Zhu, I-Ning Hu, A. Kaplan, and A. Galvanauskas, "Single-mode chirally-coupled-core fibers with larger than 50μm diameter cores," Opt. Exp. **22**, 9206-9219 (2014).
12. K. Borzycki and K. Schuster, "Arc Fusion Splicing of Photonic Crystal Fibres," in *Photonic Crystals – Introduction, Applications and Theory*, A. Massaro, ed. (InTech, 2012), pp. 175-200.
13. A. Shirakawa, H. Maruyama, K. Ueda, C. B. Olausson, J. K. Lyngsø, and J. Broeng, "High-power Yb-doped photonic bandgap fiber amplifier at 1150-1200 nm," Opt. Exp. **17**, 447-454 (2009).
14. S. S. Aleshkina, M. E. Likhachev, A. D. Pryamikov, D. A. Gaponov, A. N. Denisov, M. M. Bubnov, M. Y. Salganskii, A. Y. Laptev, A. N. Guryanov, Y. A. Uspenskii, N. L. Popov, and S. Février, "Very-large-mode-area photonic bandgap Bragg fiber polarizing in a wide spectral range," Opt. Lett. **36**, 3566-3568 (2011).

15. A. Kumar and V. Rastogi, "Design and analysis of a multilayer cladding large-mode-area optical fiber," J. Opt. A, Pure Appl. Opt. **10**(1), 015303 (2008).
16. M. Devautour, P. Roy, and S. Fevrier, "3D Modeling of modal competition in fiber laser: application to HOM suppression in multi-layered fiber," in *Conference on Lasers and Electro-Optics*(CLEO), Baltimore, MD, 2009, paper JWA.54.
17. D. Jain, C. Baskiotis, and J. K. Sahu, "Mode area scaling with Multi-trench rod-type fibers," Opt. Exp. **21**, 1448-1455 (2013). http://www.opticsinfobase.org/oe/abstract.cfm?uri=oe-21-2-1448
18. D. Jain, C. Baskiotis, and J. K. Sahu, "Bending performance of large mode area multi-trench fibers," Opt. Exp. **21**, 26663–26670 (2013). http://www.opticsinfobase.org/oe/abstract.cfm?uri=oe-21-22-26663
19. D. Jain, C. Baskiotis, T. C. May-Smith, J. Kim, and J. K. Sahu, "Large mode area multi-trench fiber with delocalization of higher order modes," [Invited], IEEE J. Sel. Top. Quantum Electron. **20**, 0902909 (2014).
20. D. Jain, Y. Jung, J. Kim, and J. K. Sahu, "Robust single-mode all-solid multi trench fiber with large effective mode area," Opt. Lett. **39**, 5200-5203 (2014).
21. J. M. Fini, "Bend-resistant design of conventional and microstructure fibers with very large mode area," Opt. Exp. **14**, 69-81 (2006). http://www.opticsinfobase.org/oe/abstract.cfm?URI=oe-14-1-69
22. Yu. A. Uspenskii, E. E. Uzorin, A. V. Vinogradov, M. E. Likhachev, S. L. Semjonov, M. M. Bubnov, E. M. Dianov, R. Jamier and S. Février, "Effect of polymer coating on leakage losses in Bragg fibers," Opt. Lett. **32**, 1202-1204 (2007).
23. J. Limpert, F. Stutzki, F. Jansen, H. J. Otto, T. Eidam, C. Jauregui, and A. Tunnermann, "Yb-doped large-pitch fibers: effective single-mode operation based on higher-order mode delocalization", [Invited], Light: Sci. & App. **1**,1-5 (2012).
24. T. Eidam, C. Wirth, C. Jauregui, F. Stutzki, F. Jansen, H.-J. Otto, O. Schmidt, T. Schreiber, J. Limpert, and A. Tünnermann, "Experimental observations of the threshold-like onset of mode instabilities in high power fiber amplifiers," Opt. Exp. **19**, 13218–13224 (2011).
25. D. Jain, C. Baskiotis, J. Kim, and J. K. Sahu, "First demonstration of single trench fiber for delocalization of higher order modes," [Contributed upgraded to Invited] " in *Conference on Lasers and Electro-Optics* (CLEO), San Jose, Calif., 2014, paper SF1N.1.
26. D. Marcuse, "Influence of curvature on the losses of doubly clad fibers," Appl. Opt. **21**, 4208-4213 (1982).
27. K. Nagano, S. Kawakani, and S. Nishida, "Change of the refractive index in an optical fiber due to external forces," Appl. Opt. **17**, 2080-2085 (1978).
28. A. W. Snyder and J. D. Love, *Optical Waveguide Theory* (Kluwer Academic Publishers, 1983).
29. J. M. Fini, R. T. Bise, M. F. Yan, A. D. Yablon, and P. W. Wisk, "Distributed fiber filter based on index-matched coupling between core and cladding," Opt. Exp. **13**, 10022-10033 (2005).
30. Z. Zhang, Y. Shi, B. Bian, and J. Lu, "Dependence of leaky mode coupling on loss in photonic crystal fiber with hybrid cladding," Opt. Exp. **16**, 1915-1922 (2008).
31. S. Saitoh, K. Saitoh, M. Kashiwagi, S. Matsuo, and Liang Dong, "Design optimization of large-mode-area all-solid photonic bandgap fibers for high-power laser applications," J. Lightwave Technol. **32,** 440-449 (2014).
32. J. M. Fini and J. W. Nicholson, "Bend compensated large-mode-area fibers: achieving robust single-modedness with transformation optics," Opt. Exp. **21**, 19173-19179 (2013).
33. C. Baskiotis, Y. Quiquempois, M. Douay, and P. Sillard, "Extending the effective area of coiled all-solid silica single-mode Bragg fibers," in ECOC, Geneva, Switzerland, 2011, paper **We.10.P1.02**.

1. Introduction

High power fiber lasers have established themselves in laser market as an attractive light source due to their outstanding features such as good beam quality, better thermal management, small foot print, and flexibility [1-2]. However, fiber laser suffers from low threshold of non-linear effects, which restrict scaling of output power [3]. One route to increase the threshold of non-linear effects is to increase the effective area (A_{eff}) of the fundamental mode (FM) of optical fiber. However, increasing the A_{eff} of the FM by increasing the core diameter leads to multimode operation and it significantly deteriorates the laser beam quality. Thus, a trade-off exists between the output power level and quality of output beam. Over the past decade, there have been numerous research efforts across the globe to find out optimum fiber designs which can offer effective single mode operation (ESM) with very large mode area (LMA). Several fiber designs have been proposed to meet ESM operation by offering high loss to the higher order modes (HOMs) such as low numerical aperture step index fiber (low NA-SIF) [4], photonic crystal fiber (PCF) [5] based designs such as leakage

channel fiber (LCF) [6], resonantly enhanced leakage channel fiber (Re-LCF) [7], and hybrid photonic crystal fiber (H-PCF) [8], photonic bandgap based fiber such as Bragg fiber [9] and 2D- all solid photonic bandgap fiber (2D-ASPBGF) [10], and resonant coupling based design such as polygonal chirally coupled core fiber (P-CCC) [11]. These designs are mostly engineered in such a way that at a practical bend radius of 10-20cm, HOMs can be suppressed by using bend induced and design based leakage loss to them. Unfortunately, inspite of their potential of offering large mode area, these designs do not fulfil the criterion for a low cost LMA fiber.

Most of these fiber designs such as PCF [5], LCF [6], Re-LCF [7], H-PCF [8], 2D-ASPBGF [10], and P-CCF [11] are difficult to fabricate because they require stack and draw process due to non-circular fiber symmetry. Moreover PCF [5], LCF [6], Re-LCF [7], H-PCF [8], Bragg fiber [9], and 2D-ASPBGF [10] require the refractive index of core and cladding to be same, which is really challenging to achieve as core of active fiber needs doping with rare earth ions and co-dopants for fiber laser operation and unfortunately these dopants are refractive index raising materials. Hence, in order to match the refractive index of actively doped core and cladding, active core is doped with additional co-dopants to reduce the core refractive index. That is why, this process dramatically increases the fabrication complexity. Moreover, these designs have their own problems such as PCF and H-PCF suffer from problem of cleaving and splicing of fibers due to presence of air holes [12], 2D-ASPBGF suffers from reduced cladding pump efficiency due to presence of high index Ge doped rods in cladding [13], and Bragg fiber suffers from unwanted coupling between core and ring modes due to imperfections in high index rings in realized fiber [14]. In addition to all these fibers, there have been several proposals of several fiber designs having additional layer or rings or tailored cladding around the core [15-16]. The suppression of HOMs is based on resonant coupling of HOMs to ring or layer or tailored cladding modes. However, these designs have limited performance. Recently, we proposed all-solid circular symmetrical design known as multi-trench fiber (MTF), which offers high loss to the HOMs induced by resonant coupling between HOMs of core and modes of resonant ring [17-18]. This design has been fabricated by using conventional fabrication process such as modified chemical vapour deposition process (MCVD) in conjunction with rod-in-tube process and results have been reported in our previous studies [19-20]. These fibers are very easy to cleave and splice thanks to the all-solid fiber structure. Unfortunately, they also require refractive index of core same as of cladding like other designs.

There is lack of standards while designing the LMA fiber design offering ESM for fiber laser applications. ESM is a relative term and depends on the chosen criterion, for example a criterion of loss of the FM lower than 0.1dB/m and HOM larger than 10dB/m was proposed by M. -Ji. Li et. al. for ESM [4]. There can be different criterion for ESM for different applications, however high loss for all the HOMs and low loss for the FM is highly preferred. Another interesting fact is that a bend radius range over which criterion is fulfilled normally depends on chosen criterion as shown in Fig. 1(a). Figure 1(a) shows that a criterion CR_1 is being fulfilled over a bend radius range of BR_1, on the other hand a criterion CR_2 is being fulfilled over a bend radius of BR_2. Furthermore, A_{eff} decreases rapidly with decreasing bend radius for LMA fiber as shown in Fig. 1(b) [21]. We define ESM for LMA at a particular wavelength as Criterion of HOM loss while low loss of FM fulfilled over a range of Bend radius with range of Effective area (A_{eff}) of the FM achieved at that wavelength, known as "CBE" {Criterion, Bend radius, Effective area}. This definition of effective single mode operation takes into account the bend radius and A_{eff}, these two parameters are very important aspects to precisely define LMA fiber for fiber laser applications. It is pertinent to note that a standard such as "CBE" is indispensable to compare the performance of various LMA fiber designs and provides useful guidance to fiber designers while designing new LMA fiber.

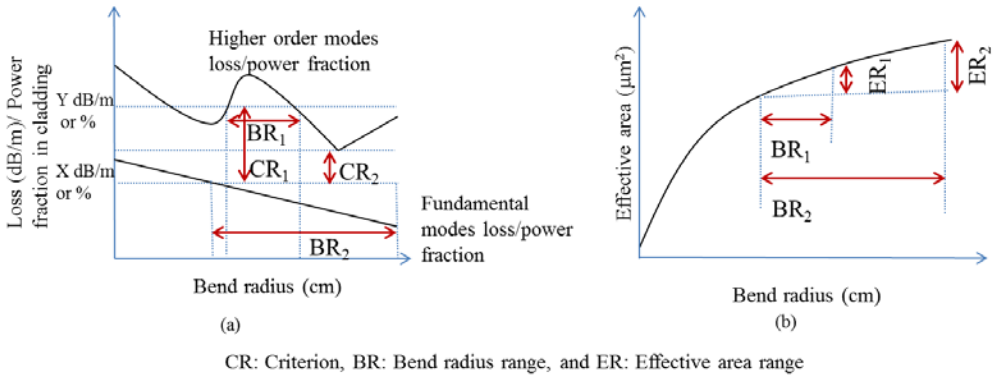

Fig. 1 (a) Loss or power fraction in cladding for FM and HOM as a function of bend radius in a LMA (b) Effective area achieved as a function of bend radius for FM.

There is another uncertainty in choosing the right criterion for ESM of LMA. Most of the fiber designs reported above are based on high loss of HOMs. However, fiber lasers are used in double cladding configuration, where the second cladding is generally a low index polymer coating (or an air-holes layer) as shown in Fig. 2(a) and this is really different from when it is generally simulated in computer world for calculating loss of HOMs as shown in Fig. 2(b). In computer simulations, an additional layer known as perfectly matched layer (PML) having same refractive index as of cladding is used in place of low index coating that is why loss calculated by simulations may not be true in reality. However, recent experiments by Gu et. al. show that asymmetrical interface between first and second cladding in double cladding case can lead to real calculated loss of core modes (as shown in Fig. 2(c)) [6]. It is worth noting that in this study by Gu et. al., the effect of cladding thickness and cladding refractive index profile were not considered [6]. A cladding diameter eight times larger than core diameter was used in this experiment [6]. On the other hand, Y. A. Uspenskii et. al. have proved the significant role of cladding layer thickness in determining the experimental loss of the FM [22] and MTFs having trench in their claddings have shown high losses for HOMs even in case of low index coated fiber [20]. Recently, researchers have stressed on the use of criterion of power delocalization of HOMs esp. in case of rod-type fiber lasers, where a small thickness of inner cladding (for example a fiber having 100μm core diameter and 170μm inner cladding diameter) is used [23]. A small cladding diameter is indispensable option to increase the cladding pump absorption in rod-type fiber lasers where fiber length is merely 1m to 2m as shown in Fig. 2(d). Moreover, the refractive index of doped core has to be equal to cladding and it becomes difficult to incorporate high amount of index raising rare earth ions and co-dopants while compensating their index with index decreasing components. Furthermore, higher suppression of HOMs can be one factor to mitigate detrimental modal instability phenomenon [24]. It is very important to note here that a small cladding diameter is not an indispensable choice in flexible fiber laser configuration inspite of the fact that most of the LMA fiber designs need same refractive index as of cladding, as a longer length of fiber can be used in fiber laser unlike rod-type fiber lasers. Nevertheless, it is important to understand that power delocalization of HOMs in flexible fiber laser configuration might not be an indispensable criterion but definitely fiber design offering this feature can dramatically enhance the performance of fiber lasers.

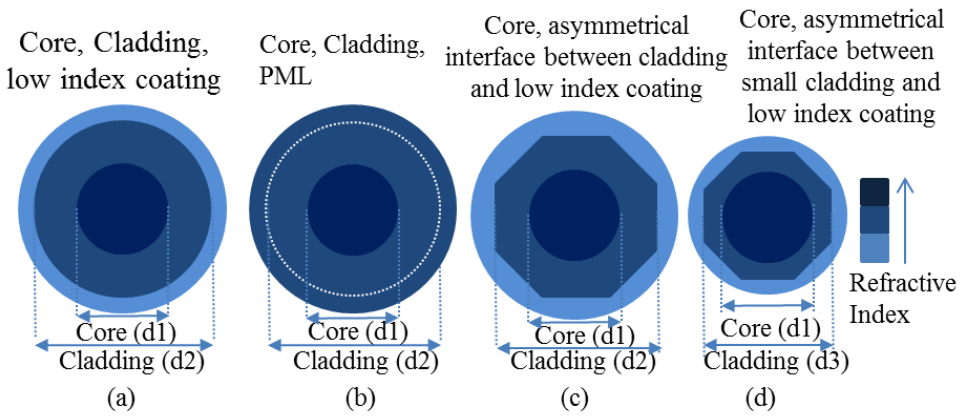

Fig. 2 Schematic of 2-D cross section of the fiber showing core and cladding with (a) low index coating (b) PML having same index as of cladding (c) asymmetrical interface of cladding and low index coating (d) asymmetrical interface of small thickness of inner cladding and low index coating.

In this paper, we report a novel fiber design which can offer circular symmetry, but more important is that the core can afford higher refractive index than the cladding. Due to this simple design, it has been fabricated with conventional active fiber fabrication process such as MCVD in conjunction with solution doping technique, hence suitable for mass production. Moreover, fiber design can offer very high delocalization of HOMs from core, in addition to the high loss. Comparative analysis based on our established definition of ESM known as "CBE" with other LMA shows significant performance enhancement. Furthermore, the proposed design is an all solid fiber structure and can be easily post processed such as cleaving, splicing, and polishing etc.

2. Single-trench fiber

We propose an optical fiber design with a core surrounded by a low and high-index ring (as shown in Fig. 3) known as single trench fiber (STF) [25]. The low index ring has same refractive index as of the cladding and high index ring has same refractive index as of the core. Figure 3(a) shows the schematic of refractive index profile (RIP) of the STF and also presents the notations used in this paper: r_c is the core radius, t is the thickness of low-index ring (trench), d is the thickness of high-index ring (resonant ring), and Δn is the refractive index difference between the core (or resonant ring) and trench (or outer cladding).

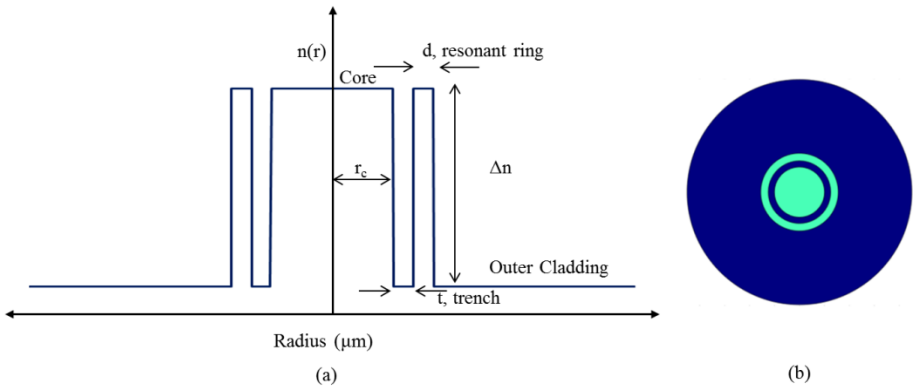

Fig. 3(a) Schematic of refractive index profile of the STF. (b) Schematic cross-section of the STF. Green and blue colours represent high and low-refractive index regions respectively.

Numerical simulations on STF shown in Fig. 3 have been performed with a full-vectorial Finite Element Method (FEM), in which the domain truncation has been ensured by using the circular anisotropic Perfectly Matched Layer (PML) as shown in Fig. 2(b). All the calculations presented in this paper are at 1.06μm wavelength. Bending losses of the STF have been analyzed using standard conformal mapping [26] with additional stress perturbations by following the standard equation:

$$n^2_{eq}(r,\varphi) = n^2(r) * \left(1 + \frac{2r}{\rho R}\cos\varphi\right),$$

where n(r) is the index profile of the unbent fiber, R is the bend radius, φ is the azimuthal angle, and ρ (here fixed to 1.25) has been included to take account of the stress factor [27].

3. Illustration of design principle of 40μm core diameter STF

Figure 4(a) shows the schematic of RIP of a low NA-SIF in unbent condition and effective RIP in bent condition. Figure 4(b) and 4(c) shows the normalized electric field of several modes in unbent and bent case respectively for core diameter=40μm, Δn=0.0005, and bent at 20cm bend radius. The leakage loss of individual modes is negligible in case of unbent condition and fiber is multi-moded. On the other hand, in bent case each mode (mainly HOMs) has significant loss due to bend induced coupling to cladding. However, the induced loss is still lower than 1dB/m for LP_{11} and the HOMs have significant power fraction in the core.

To improve the performance of low NA-SIF, we add a resonant ring around the core as shown in Fig. 4(d). The refractive index of resonant ring is same as that of the core and the region between core and resonant ring has lower refractive index that is same as that of the outer cladding. Figure 4(e) and 4(f) shows the normalized electric field of several modes in unbent and bent case respectively for STF core diameter=40μm, Δn=0.0005, t=8μm, d=6μm, and bent at 20cm bend radius. The modes of STF have negligible loss in unbent case similar to low NA-SIF case as shown in Fig. 4(b). However, the normalized electric field of modes is different from low NA-SIF case due to interaction between core and ring modes. In case of low NA-SIF we have only four guiding modes (V~4.51), on the other hand in case of STF there are nine guiding modes (first seven modes are shown here in Fig. 4(e)) including both core and resonant ring modes [28]. On the other hand, in bent case HOMs of STF have high loss compared to low NA-SIF case thanks to the bend induced resonant coupling between core and resonant ring modes [29-30]. It is well known that for a complete resonant coupling to take place between two leaky modes, there are two basic conditions to satisfy. First one is the phase matching and second one is the loss matching of two leaky modes under coupling [30]. We need to keep in mind that the modes of both core and resonant ring are leaky in bend condition and here our propose is to have high losses for HOMs of core irrespective of focusing on complete resonant coupling between core and resonant ring modes. In order to optimize the HOMs loss, we calculate the HOMs loss for different trench and resonant ring thicknesses, while keeping core diameter, Δn, and bend radius fixed to be 40μm, 0.0005, and 20cm respectively.

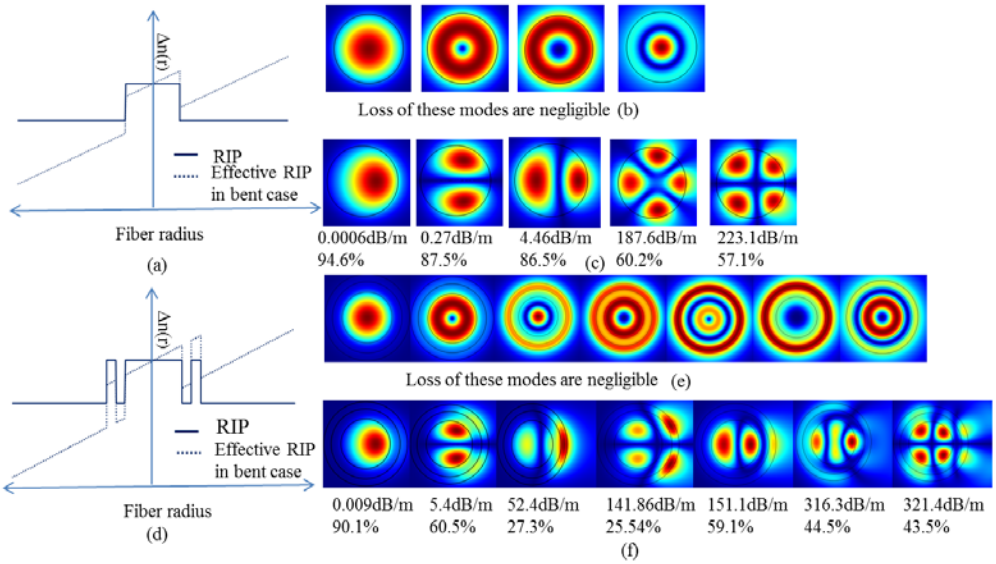

Fig. 4(a) Schematic of RIP of low NA-SIF in unbent and bent case. (b) and (c) normalized electric field of different modes in bent and unbent case with their losses and power fractions in core for 40µm core diameter SIF with Δn=0.0005 and 20cm bend radius (d) Schematic of RIP of STF in unbent and bent case. (e) and (f) normalized electric field of various modes in bent and unbent case with their losses and power fractions in core for 40µm core diameter SIF with Δn=0.0005, t=8µm, d=6µm, and 20cm bend radius.

Figure 5(a) shows the calculated loss of the FM and HOM having lowest loss among all the possible HOMs of the fiber. It includes all HOMs of core, all modes of resonant ring, mixed modes, and their polarizations. We have verified that for each resonant ring and trench thicknesses shown in Fig. 5(a), other possible HOMs (excluding FM and least lossy HOM shown in Fig. 5(a)) in fiber have loss higher than 10dB/m.

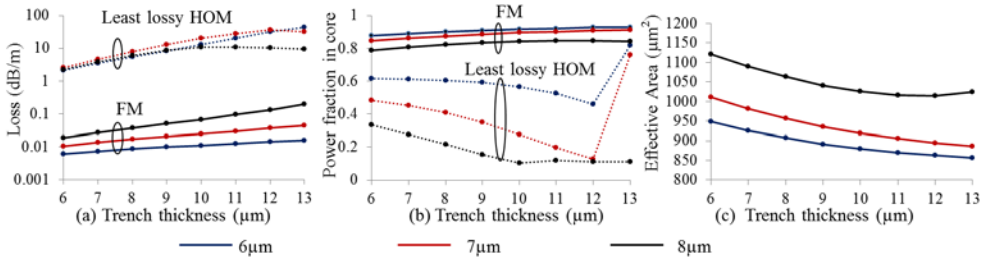

Fig. 5(a) Loss of the FM and the least lossy HOM of fiber, (b) Power fraction in core for FM and least lossy HOM of fiber, and (c) A_{eff} of the FM of fiber for different resonant ring and trench thicknesses for 40µm core diameter STF with Δn=0.0005 at 20cm bend radius.

Figure 5(b) shows their corresponding power fraction in core and Fig. 5(c) shows the A_{eff} of the FM. Table 1 also shows the loss and power fraction of the FM and other HOMs in more details. Table 1 shows that for 20 combinations (shown in red colour) out of 24 combinations of trench thicknesses t={6-13µm} and resonant ring thicknesses d={6-8µm}, the loss of the FM remains lower than 0.1dB/m and power fraction in core is higher than 80% while the loss of the HOMs are higher than 10dB/m or they have atleast 30% lower power fraction in core compared to FM or both are fulfilled simultaneously. We have verified that power fraction in core for different modes of fiber remains same even if we use low index layer in place of PML layer. The A_{eff} of the FM varies from 850µm^2 to 1120µm^2 for these 20 combinations (including bend induced distortions at 20cm bend radius). It is worth noting that for these

values of A_{eff}, the mode field diameter (MFD) comes out to be ~33µm to ~38µm from a 40µm core bent at 20cm bend radius thanks to flattening of the FM due to resonant coupling between core and ring. In nutshell, we can say that STF can offer ESM defined in term of "CBE" as criterion of loss as higher than 10dB/m for HOMs and lower than 0.1dB/m for FM or criterion of power fraction in core as higher than 80% for FM and atleast 30% lower for HOMs as compared to FM is being fulfilled at 20cm bend radius while achieving an A_{eff} of 850µm^2 to 1120µm^2 at 1060nm wavelength depending on parameters of trench and resonant ring thicknesses. The HOMs are presented in Table 1 in the order of their increasing loss. The suppression offered by STF here is extremely high, as the table contains many ring and mixed modes as well, which are very unlikely to be excited. Ring and mixed modes have low power fraction in core, although some of them may not have very high loss as of core HOMs. For example, for d=7µm and t=10µm, the FM loss and power fraction in core are 0.024dB/m and ~90% respectively, on the other hand, core HOMs (having power fraction in core larger than 50%) have loss higher than 49dB/m. Here, we can ignore ring modes having poor power fraction in core such as ~27% and ~11%.

Table 1 showing loss and power fraction in core of FM and other HOMs for different resonant ring thickness (d) and trench thickness (t).

Resonant ring thickness (d), trench thickness (t), (A_{eff} of FM)	**LP_{01} loss dB/m (power fraction in core)**	**Other HOMs loss dB/m (power fraction in core)**
6, 6 (948.72)	0.006 (0.88)	2.12(0.61), 27.08 (0.41), 68.69 (0.17), other modes>123(<47).
7, 6 (1010.71)	0.010 (0.84)	2.56 (0.48), 22.46 (0.31), 45.67(0.12), other modes>77(<62).
8, 6 (1120.07)	0.019(0.79)	2.21 (0.33), 11.29(0.28), 34.65 (0.120), other modes>45(<68).
6, 7 (925.83)	0.007(0.89)	3.46 (0.61), 38.45 (0.34), 89.24(0.12), other modes>144(<53).
7, 7 (981.26)	0.013 (0.86)	4.64 (0.45), 28.92 (0.24), 52.91 (0.08), other modes>75(<68).
8, 7 (1090.03)	0.027(0.81)	3.89 (0.28), 12.31 (0.23), 28.38 (0.08), other modes>43(<74).
6, 8 (907.02)	0.009(0.90)	5.42 (0.60), 52.38(0.27), 108.63(0.09), other modes>141(<60).
7, 8 (956.16)	0.017 (0.87)	7.94(0.41), 34.63(0.19), 59.00(0.06), other modes>72(<73).
8, 8 (1063.02)	0.037(0.82)	6.13(0.21), 12.55 (0.19), 15.69 (0.22), other modes>40(<61).
6, 9 (891.84)	0.010(0.91)	8.36(0.59), 68.34(0.21), 118.65 (0.65), other modes>124(<48).
7, 9 (935.39)	0.021(0.88)	12.95 (0.35), 38.73 (0.14), 61.10 (0.77), other modes>63(<57).
8, 9 (1041.92)	0.045 (0.83)	8.60 (0.15), 12.24 (0.16), 25.06 (0.74), other modes>35(<65).
6, 10 (879.75)	0.011(0.92)	12.91(0.57), 85.18 (0.15), 92.68 (0.71), other modes>134(<52).
7, 10 (918.54)	0.024(0.90)	19.92(0.27), 40.73 (0.11), 49.33(0.80), other modes>60(<62).
8, 10 (1025.00)	0.068 (0.84)	10.77 (0.10), 11.62 (0.13), 23.79 (0.81), other modes>30(<70).
6, 11 (870.15)	0.012(0.92)	20.19(0.52), 72.19 (0.76), 101.25 (0.11), other modes>130(<55).
7, 11 (905.084)	0.030(0.90)	28.23(0.20), 40.73 (0.08), 40.86 (0.82), other modes>51(<63).
8, 11 (1015.54)	0.093 (0.85)	10.89 (0.12), 12.24 (0.06), 20.39 (0.84), other modes>25(<74).
6, 12 (862.57)	0.014(0.93)	32.20(0.46), 56.32 (0.79), 114.60 (0.07), other modes>124(<58).
7, 12 (894.49)	0.036(0.91)	36.00(0.82), 36.05(0.13), 39.28 (0.06), other modes>40(<71).
8, 12 (1014.21)	0.13 (0.85)	10.17 (0.11), 12.93(0.04), 17.18 (0.85), other modes>21 (<77).
6, 13 (856.59)	0.01(0.93)	44.26(0.82), 51.59(0.36), 111.47 (0.44), other modes>123(<62).
7, 13 (886.34)	0.044(0.91)	31.28(0.76), 37.02 (0.05), 40.13(0.73), other modes>41(<58).
8, 13 (1024.47)	0.19(0.84)	9.52(0.11), 13.04 (0.02), 14.44 (0.86), other modes>18(<78).

In order to further investigate the suppression of the HOMs, we ignore any mode having power fraction in core lower than 50% shown in Table 1. Figure 6 depicts the loss of least lossy HOM (out of any possible mode in fiber having power fraction in core higher than 50%) and the loss of the FM for different trench and resonant ring thicknesses at 20cm bend radius. A ratio of 10^3 to 10^4 between least lossy HOM and FM can be achieved over a good range of trench and resonant ring thicknesses.

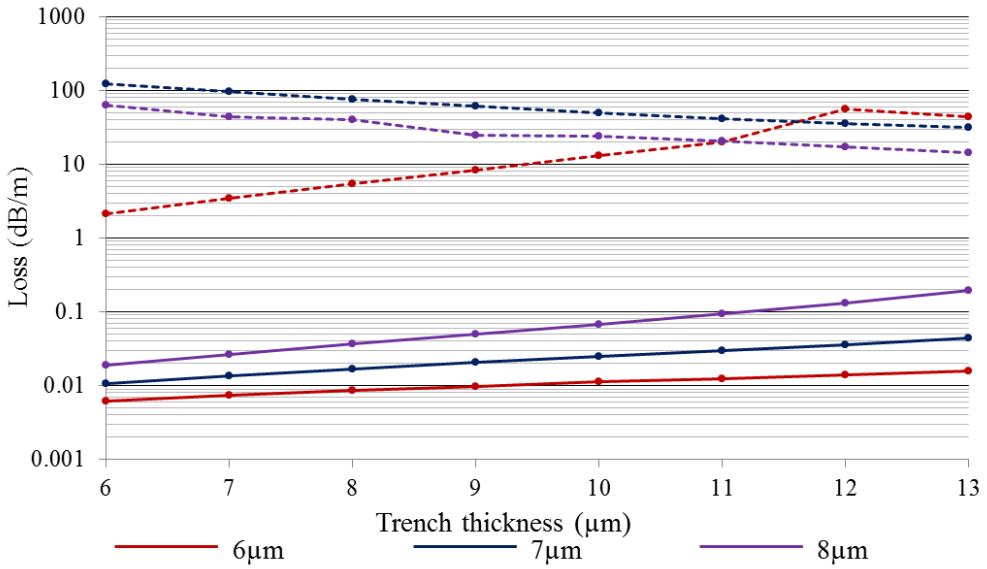

Fig. 6 Losses of the FM and the least lossy HOM of fiber. We have considered only higher order modes having power fraction more than 50% in core.

In order to further scale mode area, we investigated a STF of 50µm core diameter with Δn=0.0005 at 20cm bend radius for different ring and trench thickness. Initial simulations show that an ESM can be ensured for an A_{eff} between 1200µm^2 to 1500µm^2 depending on resonant ring and trench thicknesses. Details of numerical simulations are intended for future work.

4. Fiber fabrication and single mode behavior verification

We fabricated a Yb doped silica preform for 40µm core STF using MCVD process in conjunction with solution doping technique. The core of silica fiber is doped with Yb and other co-dopants and the silica resonant ring is doped with germanium. Figure 7(a) shows the RIP of fabricated preform having a low NA (~0.038), where slight asymmetry in preform profile is a measurement artifact only. We obtained the flat profile for core even for such a low NA using our optimized process for a long length (~400mm) of preform. Our optimized process ensures reproducibility of preform. The outer diameter of preform was 12mm, which was further etched down to 6mm using hydrofluoric acid. Etched preform was milled to have a D-shape and subsequently drawn into a fiber with cladding diameter of ~233µm. The core diameter is ~ 40µm, trench thickness (t) is ~9µm, and resonant ring thickness (d) is ~ 7µm. The fiber was coated with a low-index polymer which provided a nominal pump cladding NA of 0.48. Inset of Fig. 7(a) shows the microscope image of fiber cross-section. Core and resonant ring can be seen in microscope image of fiber. Fig 7(b) shows the white light absorption spectrum of ~1.55m long fiber and the absorption is 8dB/m at 976nm.

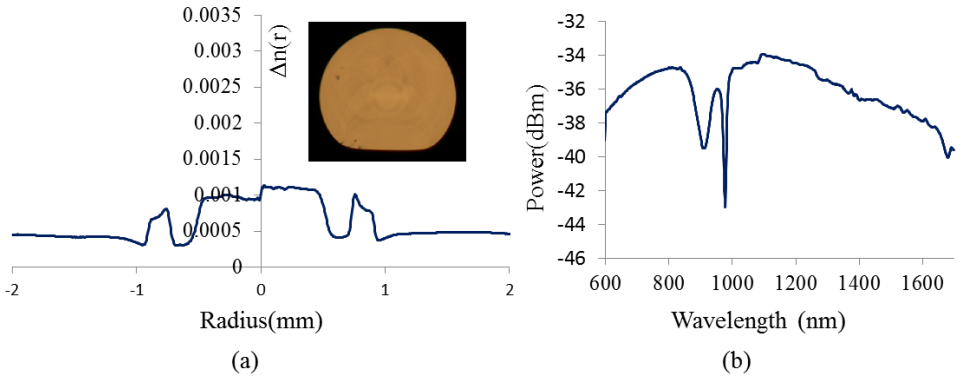

Fig. 7 (a) RIP of Yb and codopants doped preform. Inset shows the microscope image of fiber end. (b) White light absorption spectrum of a 1.55m long fiber.

Figure 8 (a) shows the experiment set-up used for verification of single mode behavior of the fiber. Here we observe the output of fiber under test (FUT) for various different input launching conditions. The aim of different launching conditions is to increase the probability of HOMs excitation. A ~1m long fabricated STF was used as FUT. We stripped the polymer coating and applied higher refractive index oil at both ends to remove cladding modes.

In order to facilitate the HOMs' excitation conditions by exploiting different modal field diameters (MFDs) and NAs of input beam and FUT, a single mode input at 1060nm wavelength was launched into FUT using a single mode fiber spliced to beam delivery fiber of laser source. Figure 8(b) shows the obtained output beam under two conditions of FUT namely loosely coiled and bent at 20cm bend radius condition, which ensures a Gaussian output beam.

In order to further enhance the multimode excitation, we use offset launching of input beam. Figure 8(c-d) show the measured power of output beam with respect to misalignment of launching beam along x-axis and output beam profiles for various offset launchings of input beam respectively. The power level of output beam with respect to misalignment of launching beam along x-axis follows a nearly Gaussian curve, on the other hand the output beams ensure a Gaussian beam output irrespective of launching conditions. It is interesting to observe from Fig. 8(d) that, only the intensity of the output beam changes but it remains Gaussian, which ensures high loss for the HOMs.

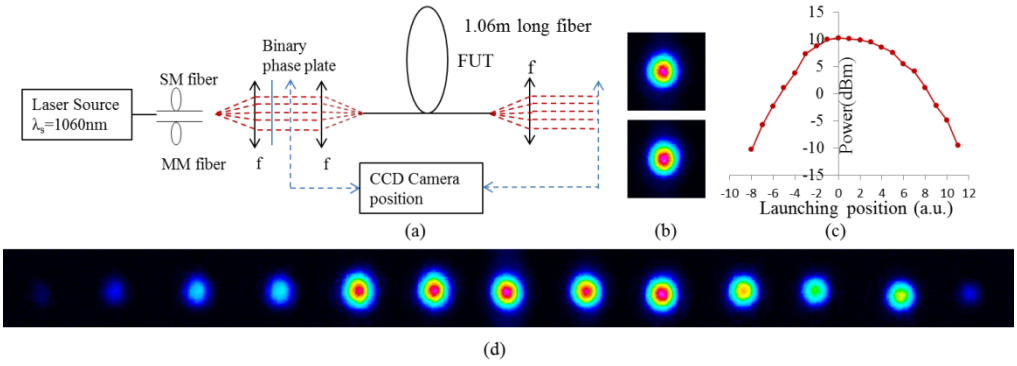

Fig. 8 (a) Experiment set-up used for single-mode characterization of STF (b) output with respect to optimum launching of single mode in loosely coiled and bent at 20cm conditions (c)

output power with respect to offset launching of single mode input (d) output beam profile with respect to offset launching of single mode input.

In order to further validate the single mode behavior of fiber, we ensured multimode input beam launch as shown in Fig. 9(a) by splicing the multimode optical fiber to the delivery fiber of 1060nm laser source, as shown in Fig. 8 (a). We again observe a Gaussian beam output as shown in Fig. 9(b), which ensures fairly robust single mode behavior of the fiber. We also generated LP_{11} and LP_{21} mode using binary phase plate as shown in Fig. 9(c-d). Figure 9(e-f) shows the output profile with respect to pure LP_{11} input beam. The output profile ensures high suppression for LP_{11} mode as we notice only residual cladding modes. Similarly, for LP_{21} launching there is no output as shown in Fig. 9(g).

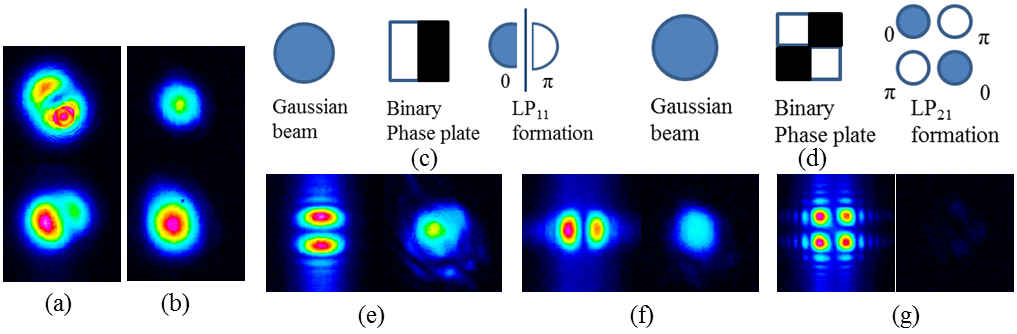

Fig. 9 (a) profile of input multimode beam (b) output beam with respect to input beam (c) and (d) binary phase plate to generate pure LP_{11} and LP_{21} mode (e) and (f) shows the output profile with respect to pure LP_{11} mode (g) shows the output profile with respect to pure LP_{21} mode.

We measured the bend loss of LP_{11} mode using ~57cm long fiber. We chose only 57cm long fiber to estimate the LP_{11} loss, as the loss of LP_{11} is high and 1m long fiber does not show any output with respect to LP_{11} launching. Figure 10(a) shows the experiment set-up used for bend loss measurement. We again use binary phase plate for LP_{11} mode launching. We first measure the output power from 57cm long fiber and change the position of fiber along different bend positions as shown in Fig. 10(a), during this movement we keep the input end of fiber fixed. Figure 10(b) shows the output power and output beam profiles of fiber placed along different bend diameters shown in Fig. 10(a). Figure 10(b) also shows the profile of output beam in straight condition, which looks like LP_{11} mode. However, with changing bend diameter of fiber the output beam profile changes rapidly and at 40cm bend diameter we notice only residual cladding modes. Moreover, output power also decreases rapidly with decreasing bend diameter. The output suffers a decrement of 10.9dB power from unbent to bent case at 40cm bend diameter; on other hand for similar study of LP_{01} mode we did not observe any considerable change in output power level.

The above mentioned results of qualitative experimental characterizations ensure a robust effective-single mode operation of FUT. It would be pertinent to note that merely 1m long length of fiber was used to verify single mode operation. Moreover, fiber has low index outer coating. In the light of these facts, it can be concluded fiber offers very high suppression to the HOMs and offers robust single-mode guidance for high power fiber laser application.

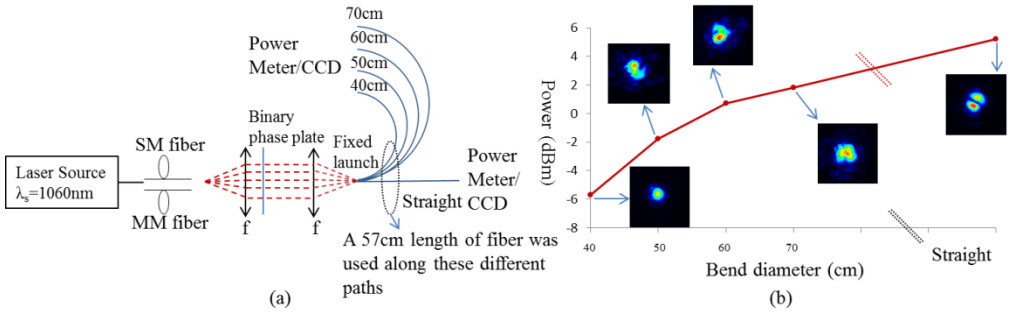

Fig. 10 (a) Experimental set-up used for calculating LP_{11} bend loss (b) output power of 57cm long fiber with respect to LP_{11} mode launch.

5. Fiber laser efficiency

We measured the fiber laser efficiency in a 4%-4% fiber laser cavity using a 3.3m long STF. Figure 11(a) shows the experimental set-up used for the laser efficiency measurement. A fiber coupled laser diode operating at a wavelength of 976 nm was used as the pump source. The pump beam was launched in to the fiber through an aspheric lens (focal length=8mm). Both ends of the fiber were cleaved perpendicularly to provide a Fresnel reflection for the laser cavity. In order to separate the signal and pump wavelengths, a dichroic mirror with high reflection at pump wavelength and high transmission at signal wavelength was used at the pump launch end. At the pump exit end of the fiber under test (FUT), output beam was collimated and focused using aspheric lens (focal length=8mm) and a dichroic mirror with high transmission at pump wavelength and high reflection at signal wavelength was used to separate signal and pump wavelengths. Figure 11(b) shows the measured slope efficiency with respect to launched power, a ~75% slope efficiency was obtained. Inset show the obtained profile of output beam and a M^2 of ~1.15 was obtained for output beam. Figure 11(c) shows the measured spectrum of output beam at different power level, showing laser output at ~1040nm.

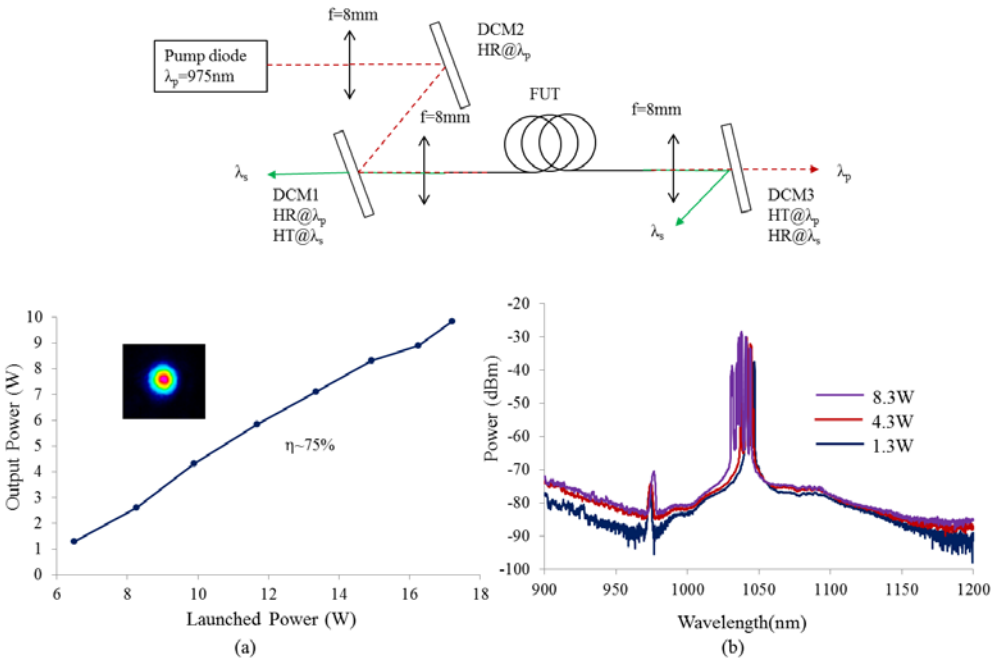

Fig. 11 (a) Experimental set-up used for fiber laser efficiency (b) slope efficiency of 3.3m long fiber. Inset shows the profile of output beam (c) measured spectrum of output beam at different power levels.

6. Comparison with other LMA

As we mentioned in the introduction there are numerous fiber designs proposed by fiber community such as Low NA-SIF, H-PCF, LCF, 2D-LCF, 2D-ASPBG, Bragg fiber, P-CCC, and bend compensated parabolic fiber. In this section, we do a fair comparison for different fiber designs with STF on different aspects of fiber design such as A_{eff} for ESM, fiber structure such as solid structure or not, cylindrical symmetrical or not, and refractive index of core higher than cladding or not. A fair comparison of different fiber designs is usually a challenging task. That is why, here we use our definition "CBE" of ESM for comparison of different fiber designs. We fix here three parameters: first is criterion in term of loss as minimum 10dB/m loss for HOMs and maximum 0.1dB/m loss for FM, second is maximum bend radius of 20cm, and third is the operating wavelength ~1060nm to compare A_{eff} achieved for different fiber design. Table 2 shows the A_{eff} achieved for different fiber design, their structure such as solid structure or not, cylindrical symmetry or not, core refractive index higher than cladding or not. It is necessary to mention few points here about different designs in comparison table; which have not been possible to mention in table. We ignore LCF because Re-LCF has been reported to have better performance with slight changes in features of LCF fiber design [6, 7]. 2D-ASPBGF can provide A_{eff} in range of 1000-1400μm^2, however as A_{eff} increases from 1000μm^2 to 1400μm^2 the mode suffers rapid distortion. Distortion or illuminated fraction of a mode can be defined as ratio of A_{eff} of the FM in bent condition (here it is 20cm bend radius) to A_{eff} of the FM in straight condition. In case of 2D-ASPBGF, the black fraction of the FM drops from 0.67 to 0.30 for 1100μm^2 to 1400μm^2 A_{eff} [31]. On the other hand, P-CCC fiber has been reported with ~55μm to ~60μm core [11]. However, the bending performances of FM and HOMs loss and the A_{eff} of the FM in bend configuration

have not been reported, which is extremely important to show a substantial candidature for fiber laser applications. That is why, it is not possible to report A_{eff} here for P-CCC, hence we just mention about their structural aspects. In case of bend compensated parabolic fiber, the A_{eff} ~1000μm^2 is numerically reported at 15cm bend radius, which is a spectacular performance [32]. However, this design requires a high precision in controlling the doped RIP of fiber on ~10^{-4} level, which might be challenging to achieve.

Table 2 Comparison of different fiber designs.

Fiber Design	**Maximum A_{eff}** (FM 0.1dB/m & HOM >10dB/m)	**All-solid**	**Cylindrical symmetrical**	**Core index higher than cladding**
Low NA-SIF [4]	~370μm^2	Yes	Yes	Yes
Re-LCF [6,7]	~900μm^2	Yes	No	No
2D-ASPBGF [10, 31]	~1,000-1,400μm^2	Yes	No	No
Bragg Fiber [33]	~1,020μm^2	Yes	Yes	No
P-CCC [11]	Not provided	Yes	No	Yes
Bend compensated Parabolic fiber [32]	~1,000μm^2	Yes	Yes	Yes
STF [current work]	~1,000-1,500μm^2	Yes	Yes	Yes

7. Conclusion

We propose a novel fiber design single-trench fiber (STF) for large mode area fiber laser and amplifier. STF offers cylindrical symmetry as well as higher refractive index of core compared to cladding. This avoids the need of stack and draw process and refractive index compensation of core doped with index raising rare-earth and co-dopants ions, which are indispensable conditions in case of LCF, Re-LCF, and 2D-ASPBGF. STF design can be fabricated with conventional MCVD process in conjunction with solution doping process, which can dramatically reduce the fabrication cost, hence suitable for mass production. All-solid structure of STF ensures easy cleaving and splicing. Fiber can offer very high loss (>10dB/m) and low power fraction in core (<50%) to the higher order modes for low loss of FM (<0.1dB/m) and high power fraction in core (>80%) for A_{eff} as large as 1,000μm^2 at ~1060nm thanks to the resonant coupling between core and ring modes.

A 40μm core Yb-doped STF was fabricated using MCVD process in conjunction with solution doping process in a single step, without using any micro-structuration and pixilation of core. Experiments ensure the robust single mode behaviour irrespective of launching condition of input beam and offering good laser efficiency at ~1040nm. A comparative analysis of STF with other designs such as Low-NA SIF, Re-LCF, 2D-ASPBGF, P-CCC, and

Bragg fiber shows significant performance enhancement, in addition to several other advantages offered in terms of low cost, large-scale production, and easy post-processing of fibers, thanks to simple fiber design.

Acknowledgments

The work is supported by the EPSRC Centre for the Innovative manufacturing in Photonics EP/HO2607X/1.